14 January 1983, Volume 219, Number 4581 SCIENCE

Cosmic-Ray Record in Solar System Matter

Robert C. Reedy, James R. Arnold, Devendra Lal

The earth moves in a region of space once thought of as empty. The density of ambient gas is low, though measurable, as is the density of solar thermal photons, 3 K universal black body photons, and other low-energy particles. In this article we discuss the fluxes of high-energy nuclear particles in the earth's neighborhood, the inner solar system.

We define high-energy particles as those with energies on the order of 1 million electron volts or more per nucleon and consider only two types of energetic particles in the earth's environment: the galactic cosmic rays (GCR), which come from outside the solar system, and the solar cosmic rays (SCR), emitted irregularly by major flares on the sun. These particles have sufficient energy to penetrate deeply into solids and to interact with them, and they produce appreciable chemical effects, atomic displacements, and ionization in suitable media. Particles with higher energies, above ~ 10 megaelectron volts, also produce nuclear reactions. Because these various effects leave persistent records, the study of our high-energy particle environment is rich in historical possibilities.

It is easy to study solar and galactic cosmic rays separately. The GCR particles have high energies and are continuously incident on the solar system, but their flux and energy spectrum is modulated by solar activity. They produce effects to considerable depths, and are therefore important in larger bodies. The sporadic SCR particles, on the other hand, have much lower energies but higher average fluxes; the distinctive effects due to solar particles can be seen in the surface layers of extraterrestrial matter.

Summary. The energetic nuclei in cosmic rays interact with meteoroids, the moon, planets, and other solar system matter. The nuclides and heavy nuclei tracks produced by the cosmic-ray particles in these targets contain a wealth of information about the history of the objects and temporal and spatial variations in the particle fluxes. Most lunar samples and many meteorites have complex histories of cosmic-ray exposure from erosion, gardening, fragmentation, orbital changes, and other processes. There appear to be variations in the past fluxes of solar particles, and possibly also galactic cosmic rays, on time scales of 10^4 to 10^7 years.

The records of both types of particles have been studied in terrestrial as well as extraterrestrial samples, such as meteorites and lunar rocks and soils. To study cosmic rays, the irradiation history of extraterrestrial samples and the transport processes on the earth must be understood. Although it is possible to study the history of asteroidal and planetary surface processes by studying the effects of charged-particle irradiation, this is a bootstrap process, involving studying one with assumptions about the other. The big differences in the nature and the interactions of the two types of cosmic-ray particles, the availability of a suite of terrestrial and extraterrestrial materials, and significant technological developments in studying the effects of charged-particle irradiation, have made it possible in the last decade to make significant progress in both fields.

Nature of the Cosmic Rays

The energetic nuclei in the solar system have a vast variety of energies and compositions (Table 1). The nuclei in both the GCR and SCR are mainly protons and alpha particles (ratio ~ 10 to 20), with about 1 percent heavier nuclei (lithium to atomic number Z ~ 90 or more). The cosmic-ray intensities vary with geomagnetic latitude and with solar phenomena (*1*). Alterations in the mean flux of solar particles, and in the GCR flux, are both tied to the 11-year sunspot cycle (*1, 2*). Near sunspot maximum, the GCR flux decreases whereas the mean intensity of particles emitted by solar flares increases. Although these and other properties of cosmic rays were established by earth-based observations, measurements from spacecraft, especially beyond 1 astronomical unit from the sun, have refined and extended our knowledge of the origin, nature, and distribution of these energetic particles (*2*).

The initial sources of the GCR particles and the mechanisms for their acceleration are not known well but probably involve supernovae (discrete sources), the interstellar medium (diffuse sources), or both (*3*). As the particles diffuse or are transported to the solar system, various interactions, including acceleration, may occur. Finally, the solar magnetic fields modulate the spectrum of GCR particles as the particles enter the heliosphere zone, which extends out to ~ 50 AU. The modulation is due to scattering of particles on irregularities in the interplanetary magnetic fields, which are convected outward by the highly conductive solar wind plasma (*4*). Although changes in the sources, acceleration, or interstellar propagation of the particles can change their fluxes in the solar system, solar modulation is the dominant source of the observed GCR variability (Fig. 1).

The fluxes of 200 to 500 MeV particles

Robert C. Reedy is a staff member in the Nuclear Chemistry Group, Los Alamos National Laboratory, Los Alamos, New Mexico 87545, and is currently a visiting scientist at Max-Planck-Institut für Chemie, D-6500 Mainz, Federal Republic of Germany. James R. Arnold is a professor in the Department of Chemistry, University of California at San Diego, La Jolla 92093, and director of the California Space Institute. Devendra Lal is the director of the Physical Research Laboratory, Navrangpura, Ahmedabad 380009 India, and visiting professor at Scripps Institution of Oceanography, La Jolla, California 92093.

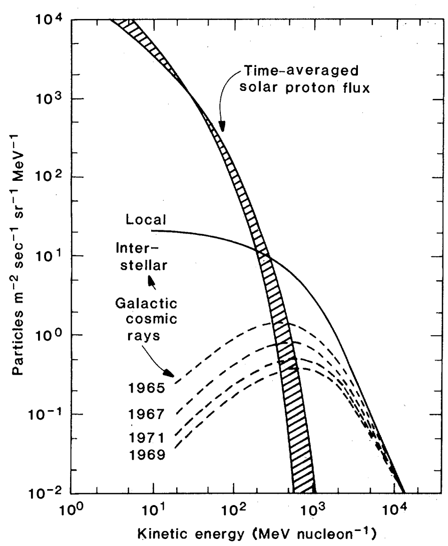

Fig. 1. The long-term average fluxes of solar protons determined from lunar data and GCR-proton fluxes for different modulation levels. The fluxes of GCR protons near the earth for 1965, 1967, 1969, and 1971 are calculated fits to satellite data and the curve for local interstellar space was estimated from modulation theory (*75*). [GCR curves and calculations courtesy of M. Garcia-Munoz and J. A. Simpson]

are modulated by an order of magnitude during a solar cycle. At $E > 5$ to 10 gigaelectron volts per nucleon, the spectrum of GCR particles is not influenced much by solar activity, and its shape can be described roughly by a power law in energy, $E^{-2.5}$. Most nuclear interactions that produce records are induced by particles with $E > 1$ GeV per nucleon, which are affected only slightly by solar modulation.

An important question in examining the cosmic-ray record is how the GCR spectra varied during sustained periods of low or high solar activity. During long periods of essentially no solar activity, such as the Maunder minimum from 1645 to 1715 (*5*), the GCR particles would not be hindered from reaching the inner solar system. The local interstellar spectrum (*6*) is estimated (*7*) to be similar to the one that is in the inner solar system during such periods of low solar activity.

At a distance of 1 AU from the sun, solar flare particles constitute an important source of medium energy (< 100 MeV per nucleon) corpuscular radiation. More than 100 solar flare cosmic-ray events have been observed near the earth since 1950. Only a few large flares produce most of the SCR particles emitted during an 11-year sunspot cycle (Fig. 2). When solar activity is low (sunspot numbers below 50), few energetic particles are emitted. The fluence of protons with $E > 10$ MeV in individual events has ranged from below 10^5 to more than 10^{10} protons per square centimeter (*8, 9*). Individual events last for a couple of days and have time-averaged fluxes that are several orders of magnitude higher than the total GCR flux.

The energy spectrum of solar particles is soft, with many particles of $E > 10$ MeV but few with $E > 100$ MeV. In general, the spectrum of SCR particles can be represented fairly well by $E^{-\gamma}$, where E is the kinetic energy per nucleon. For proton energies between 20 and 80 MeV γ typically ranges from 2 to 4, with an average of 2.9 at the time of maximum proton intensity (*10*). For $E < 20$ MeV, γ is generally lower and for $E > 100$ MeV the energy spectrum is usually steeper. Several other spectral shapes are also used for solar protons (*9*).

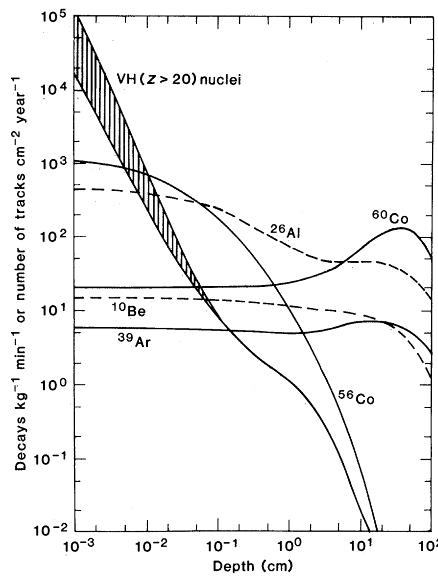

Fig. 3. Predicted production rates for heavy-nuclei tracks and various radionuclides as a function of depth in a lunar rock (density of 3.4 g cm^{-3}) directly exposed to cosmic-ray particles. The shaded region reflects uncertainties in the fluxes of low-energy VH nuclei in the SCR (*16*). The units for the production of ^{60}Co by the ^{59}Co(n,γ) reaction (*76*) are disintegrations per minute per gram of cobalt. The other curves were calculated by the Reedy-Arnold model (*11*) and the chemical composition of lunar rock 12002. The curve for ^{56}Co represents only production by solar protons by the ^{56}Fe(p,n)^{56}Co reaction. For ^{26}Al, ^{39}Ar, and ^{10}Be, production by both solar protons and GCR particles were included, although solar proton production is important only for ^{26}Al.

Cosmic-Ray Particle Interactions with Matter

The energy, charge, and mass of an energetic particle and the mineralogy or chemistry of the target mainly determine which interaction processes are important and which cosmogenic (cosmic ray–produced) products are formed. Energetic nuclear particles mainly interact with matter in two ways (*11*). (i) All charged nuclei continuously lose energy by ionizing atoms as they pass through matter, and the damage produced by radiation can accumulate in matter and be detected as thermoluminescence. The paths traveled by individual nuclei with $Z > \sim 20$ and with energies from 0.1 to 1 MeV per nucleon can be etched by certain chemicals and made visible as tracks (*12*). (ii) A nuclear reaction between an incident particle and a target nucleus involves the formation of new, secondary particles (for example, neutrons, pions, and gamma rays) and of a residual nucleus which is usually different from the initial one. Nuclei of low energy and high Z lose energy rapidly through ionization and come to rest. Those of high energy and low Z lose energy more slowly and usually induce nuclear reactions before stopping.

Because of the variety of the cosmic-ray particles and of their modes of interaction, the effective depths and products of the interactions vary considerably (Table 1). Below a depth of ~ 1000

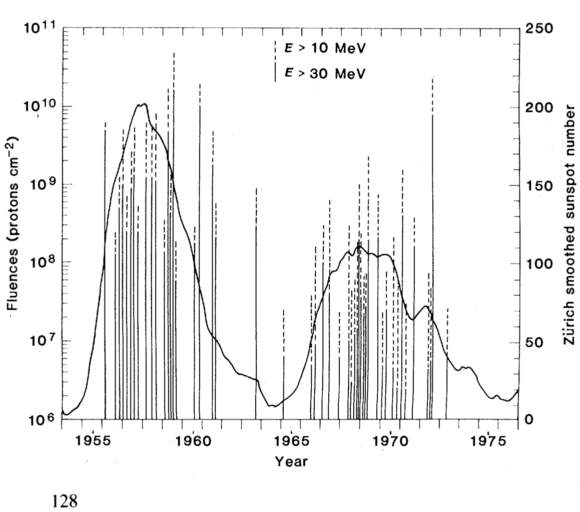

Fig. 2. Zürich smoothed sunspot number (continuous solid curve) and the omnidirectional integral fluxes of protons above 10 and 30 MeV emitted by solar flares from 1954 to 1976. Fluences for several flares that occurred close to each other have been combined (*8*).

grams per square centimeter (a few meters in solid matter or the thickness of the earth's atmosphere) there are few cosmic-ray particles; most have been removed by nuclear reactions or stopped by ionization.

Collisions with large meteoroids can reduce or destroy the part of an extraterrestrial object that was exposed to cosmic-ray particles and expose new surfaces. Erosion rates due to microcratering are $\sim$ 1 millimeter per 10^6 years for most exposed rocks. The simultaneous study of implanted solar wind ions, solar and galactic heavy nuclei tracks, and nuclides produced by GCR and SCR nuclei can reveal changes in the irradiation geometry because each of these effects has a characteristic depth dependence.

When extraterrestrial matter is exposed to cosmic rays, a wide variety of cosmogenic stable and radioactive nuclides are made. The important targets for cosmic ray–induced reactions are the common elements like oxygen, magnesium, silicon, and iron. The mass of product nuclides is similar to or less than that of the target nucleus. Half-lives of frequently measured cosmogenic radionuclides range from a few days (35 days for ^{37}Ar) to millions of years (3.7×10^6 years for ^{53}Mn). The activity of a cosmogenic radionuclide starts near zero for a freshly exposed sample and will approach its production rate (assumed to be constant) after the sample has been exposed to cosmic rays for several half-lives. Stable cosmogenic noble gas nuclides, such as ^{21}Ne, are readily detected by mass spectrometry and are often used to determine a sample's integral exposure to cosmic rays.

The relatively low-energy solar protons and alpha particles are usually stopped by ionization energy losses near the surface of extraterrestrial matter. The SCR particles that induce nuclear reactions produce few secondary particles (and the product nucleus is close in mass to the target nucleus). Nuclear reactions induced by SCR-produced secondary neutrons are unimportant (*13*). The fluxes of SCR particles as a function of depth can be calculated accurately from ionization–energy loss relations; thus production rates of a nuclide as a function of depth can be calculated well if the cross sections for its formation are known. Activities of SCR-produced nuclides decrease rapidly with increasing depth (^{56}Co in Fig. 3).

Because high-energy GCR particles have ranges in matter that are much longer than their interaction lengths, most react before they are stopped, and each reaction with a nucleus usually produces many secondary particles, especially neutrons and pi mesons. The cascade of particles that develops from these interactions produces a population with many low- and medium-energy particles. The fluxes of the incident GCR particles decrease roughly exponentially with depth. The fluxes of secondary neutrons increase with depth near the surface, but then decrease exponentially with depth (*11*). In large objects, many secondary neutrons are slowed by scattering reactions to low energies and can produce certain nuclides, like ^{60}Co, by neutron capture reactions (*14*). The spectrum of the particles in an extraterrestrial object varies with depth and with the size of the object. Although the flux of GCR particles varies with solar activity, the shapes of their production rate-depth curves do not change much during a solar cycle (*13*).

Table 1. Energies, mean fluxes, and interaction depths of various types of cosmic-ray particles.

Radiation	Energies (MeV nucleon^{-1})	Mean flux (particles cm^{-2} sec^{-1})	Effective depth (cm)
	Solar cosmic radiation		
Protons and helium nuclei	5 to 100	$\sim$ 100	0 to 2
Iron group and heavier nuclei	1 to 50	$\sim$ 1	0 to 0.1
	Galactic cosmic radiation		
Protons and helium nuclei	100 to 3000	3	0 to 100
Iron group and heavier nuclei	$\sim$ 100	0.03	0 to 10

The nature of the cascade caused by GCR particles and the resulting spectrum is well known from theoretical calculations (*13, 14*), bombardments of thick targets with accelerated particles (*15*), and studies of cosmogenic nuclides in extraterrestrial objects (*9, 11*). Because both the attenuation of primary GCR particles and the build up of secondary particles occur gradually as a function of depth, the depth-activity profile of a GCR-produced nuclide varies slowly (Fig. 3) and depends on the excitation functions (cross sections as a function of energy) of the reactions producing it (*11*); compare, for example, ^{39}Ar and ^{10}Be. Below a depth of about 100 g/cm^2 (about 300 g/cm^2 for neutron-capture reactions), the production rates of GCR-produced nuclides decrease with depth with an *e*-folding length of about 200 g/cm^2 (*11, 14*). The big difference in the depth-activity profiles for the production of nuclides by SCR and GCR (Fig. 3) usually allows these two components to be resolved.

Although nuclear reactions can occur in all the constituent phases of meteorites and lunar samples, observations of solid-state damage due to charged particle irradiation are usually limited to the crystalline dielectric phases of the minerals present, usually olivines, pyroxenes, and feldspars. Various techniques are used to observe solid-state damage due to solar wind , heavy cosmic-ray nuclei (usually $Z > 20$), and fission fragments (*9, 12*). We are primarily concerned here with tracks due to cosmic-ray nuclei of $Z \geq 20$. From their observed abundances, these nuclei are conveniently divided into two groups, those with $20 < Z \leq 28$, the iron or VH group, and the $Z \geq 30$ nuclei, the VVH group. The VVH nuclei (mainly, $30 \leq Z \leq 40$) are less abundant than the VH nuclei by about a factor of 500 to 700 for energies above $\sim$ 500 MeV per nucleon (*16*). The determination of Z for the nucleus forming a track can now usually be made within ± 2 charge units (*12, 16*). The identification of charge group (VH or VVH) can be made with certainty.

Profiles of track density as a function of depth have been determined in many meteorites and lunar samples with simple exposure histories and in a number of man-made materials exposed in space, including a glass filter from the Surveyor III camera returned by the Apollo 12 astronauts. In a track production profile for the moon (Fig. 3), the tracks in the top $\sim$ 1 mm are made mainly by heavy SCR nuclei ($E < \sim 10$ MeV per nucleon); the deeper tracks are made by GCR nuclei ($E \geq 100$ MeV per nucleon) after they have slowed to $E \sim 2$ MeV per nucleon.

History of the Targets

The record of the effects of cosmic-ray bombardment on the earth and in lunar rocks and soil, meteorites of various classes, interplanetary dust collected in the stratosphere, and cosmic spherules found in deep-sea sediments is discussed in the following paragraphs. For these materials, the study of cosmogenic nuclides and nuclear tracks gives significant historical information.

Earth. The most famous cosmogenic radionuclide is ^{14}C (*17*), whose half-life is 5730 years. On the shortest time scales

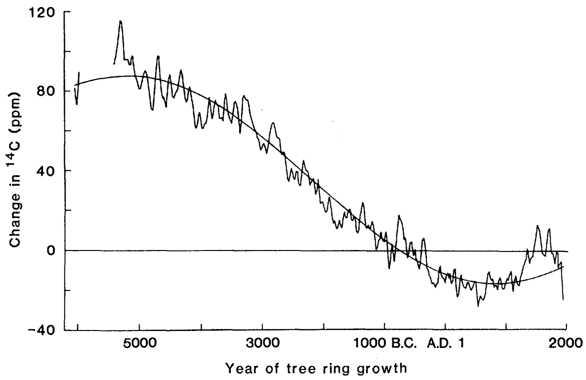

Fig. 4. Best-fit sine curve and spline functions drawn through the experimental change in ^{14}C values measured in parts per thousand at the La Jolla Radiocarbon Laboratory for dated tree rings (*19*). The 10^4-year sine curve represents the slow variation caused by the changing geomagnetic field. The high frequence fluctuations (Suess wiggles) are computer-generated spline functions through the experimental $\Delta^{14}C$ variations. [Courtesy of H. E. Suess (*19*)]

accessible to ^{14}C—tens to hundreds of years—correlations are observed among solar activity indices, climatic variables (especially temperature), and ^{14}C activity. When sunspots are few, ^{14}C activity is relatively high, and the climate is generally cold (*5, 18–20*). The higher ^{14}C content can be understood as a consequence of more GCR protons reaching the earth. It is less clear how solar activity affects climate.

In the 10^3- to 10^4-year range the dominant effect seems to be variation in the earth's magnetic field (Fig. 4). The main dipole field was apparently weaker one to two ^{14}C half-lives ago, so that more protons reached the earth, and the ^{14}C production rate was higher. The effect is modeled as a sinusoidal variation, with an amplitude in ^{14}C of about 10 percent and a period of about 10^4 years (*18*). Because only the last half-cycle is subject to detailed check, the true variation curve may not be close to the model at times further back than 10^4 years.

Longer-lived cosmogenic radionuclides enter the terrestrial environment in at least three ways. They are carried in by meteoritic material bombarded in space. This is the main source of nuclides produced from iron-group targets in meteorites, the most important of which is ^{53}Mn, with a half-life of 3.7×10^6 years. They are also produced by spallation reactions in the atmosphere; ^{10}Be (half-life, 1.6×10^6 years) is made from oxygen and nitrogen in this way (*21*), and bombardment of atmospheric argon is the main source of ^{26}Al (half-life, 7×10^5 years) (*22*). Finally, a small amount of production takes place in surface rocks and soil because of reactions of neutrons and muons.

Sensitive methods of detection, such as activation analysis for ^{53}Mn (*23*) and the use of accelerators for high-energy ion counting (*24*), have increased interest in these nuclides. For example, interest in ^{53}Mn is related to understanding the special processes that lead to the deposition of manganese-rich nodules and crusts in the deep sea. Raisbeck and coworkers (*25*) have measured the ^{10}Be content of seawater, ice cores, and sediments. We expect this work to lead to the development of models of the distribution of ^{10}Be in natural waters and sediments, which will permit this nuclide to play a useful role in geochronology and geochemistry. The chemical similarity of beryllium and aluminum suggests that atmospheric ^{10}Be and ^{26}Al should be distributed in the same way. Measurement of the $^{26}Al/^{10}Be$ ratio can provide another parameter and reduce the need for a well-supported geochemical model.

Moon. Because the moon has no atmosphere and relatively weak magnetic fields, cosmic rays produce all their effects in solid matter. Transport and mixing are slow by terrestrial standards. The transport process of "gardening" (regolith turnover) by meteoritic impact seems to predominate at the scales of distance and time accessible to our study. The radionuclides ^{53}Mn and ^{26}Al, produced abundantly by solar protons at depths less than a few centimeters, are ideally suited for gardening studies on a time scale of 10^6 to 10^7 years.

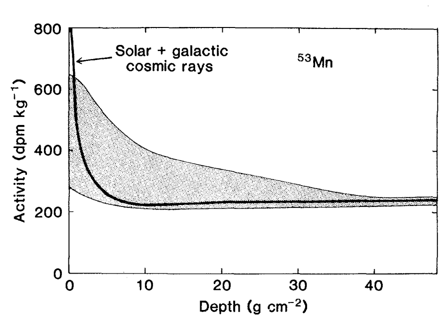

Fig. 5. Activity profile of ^{53}Mn in disintegrations per minute of ^{53}Mn per kilogram of iron. The heavy line is a calculated production profile for ^{53}Mn as a function of depth from the model of Reedy and Arnold (*11*) and parameters determined from lunar rock data. The hatched region covers the experimental ^{53}Mn concentrations determined in seven lunar cores (*77*). The broad spread results from the varying degrees of disturbance (gardening) which have occurred at the different places sampled, on a time scale of $\sim 10^7$ years. To convert the depth scale to centimeters, divide by ~ 1.8.

Our collections contain basically two kinds of samples. Rocks collected on the surface have been there for at least 10^6 years, with interesting exceptions. Most rocks seem to have had complex surface histories (*26*), in which tumbling, fragmentation, burial, and reexposure have all played a role. It also seems clear that on time scales as long as 10^7 years, a simple one-stage bombardment history on the moon's surface is improbable for rocks small enough to be collected. One well-characterized event, formation of the South Ray crater at the Apollo 16 site 2.0×10^6 years ago (*27*), ejected pristine material from below the zone penetrated by cosmic rays, including some rocks with simple bombardment histories. The dominant alteration effect in such rocks is erosion, produced mainly by sandblasting by micrometeorites, at a rate of ~ 1 mm per 10^6 years (*9*). The rate is dependent on the hardness of the rock.

The most instructive samples of the lunar regolith or soil are cores, ranging in length from about 20 cm to 3 m. Their history also appears to be complex, involving usually one or a few large cratering or depositional events, superimposed on a quasi-continuum of smaller disturbances. The nuclear track data (*9, 12, 16*) make clear the local heterogeneity of each layer, except for rare materials like the Apollo 17 orange glass. The lunar core track results also suggest several episodic enhancements in meteorite bombardment rates (*28*) during the last $\sim 10^9$ years. The data on SCR-produced ^{53}Mn (Fig. 5) and ^{26}Al show that disturbance has occurred, on a time scale of 10^6 to 10^7 years, to a depth that varies from a few to more then 10 cm. The deeper layers are undisturbed on this time scale. Monte Carlo models give a fairly satisfactory match with such observations (*29*).

Meteorites. Cosmogenic noble gases, radionuclides (especially ^{53}Mn and ^{26}Al), and tracks measured in meteorites are the main source of evidence that most or all classes of meteorites originate in the asteroid belt, between Mars and Jupiter. The production rates for cosmogenic nuclides or tracks as a function of composition and shielding conditions (preatmospheric size and sample location) are known fairly well and are often used to determine the duration of exposure of a meteorite to cosmic-ray particles.

The exposure (or bombardment) age of a meteorite is most precisely measured with a radionuclide–stable product pair. The activity of the radionuclide is used to determine the production rate of the stable nuclide. The best pair is ^{81}Kr-^{83}Kr because both nuclides are produced by closely similar reactions, and both are measured by mass spectrometry at the same time. For long-lived iron meteorites, the measurement of ^{40}K (1.26×10^9 years) along with stable cosmogenic potassium isotopes is of great value (*30*). More commonly, a production rate for ^{21}Ne or some other nuclide is used. Recently, ^{22}Ne/^{21}Ne isotopic ratios in meteoritic samples have been used to correct ^{21}Ne production rates for the shielding conditions during exposure of the samples (*31*). Nuclear tracks and activities of long-lived radionuclides also provide information on the exposure history of meteorites. There have been uncertainties about the actual exposure ages (*32, 33*), but the ^{21}Ne data yield a good set of relative ages.

Bombardment ages of chondritic meteorites range up to a few tens of millions of years (*34*) (Fig. 6); those of iron meteorites are longer (*30*). The longest bombardment age so far, about 2×10^9 years on the ^{40}K-^{41}K scale, is that of the iron meteorite Deep Springs (*30*). There are statistically significant groups of H-group chondrites at 4×10^6 to 8×10^6 years (Fig. 6), and of coarse octahedrites (irons) at 5×10^8 to 6×10^8 years. These groupings, associated with specific meteorite types, appear to record individual events. Our picture is that meteorites spent their earlier histories contained in bodies that were large in comparison to the characteristic length of GCR penetration, a few meters. The start of the cosmic-ray exposure was a collision between two objects, which produced disruption or at least fragments of meteoritic size. These were brought into earth-crossing orbits by planetary perturbations (*35*). The observed time scales and age groupings have been essential data for the development of planetary perturbation models.

Some meteorites have been small objects for a relatively short time. The extreme example, so far, is the chondrite Farmington (*36*), with a bombardment age of 5×10^4 years. There is little time for perturbation of the orbit of such a short-lived object; thus if the orbit could be determined, it would be of major importance.

Multistage bombardments in space were noted by Chang and Wänke (*37*) for large iron meteorites. For such objects, 1 m or larger with bombardment ages $\sim 5 \times 10^8$ years, two or more stages of collisional breakup seem to be the rule. Nishiizumi (*38*) reported two cases, one very striking, of two-stage bombardment of chondrites in space.

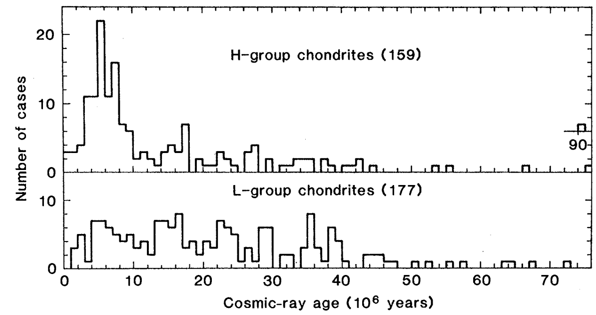

Fig. 6. Cosmic-ray exposure ages of the major types of stone meteorites calculated from measured concentrations of cosmogenic ^{21}Ne and ^{22}Ne/^{21}Ne ratios (for shielding corrections) taken from various sources. [Courtesy J. Smith and K. Marti]

There is evidence for precompaction irradiation—that is, the exposure to high-energy radiation preceding the assembly of the meteorite as a solid rock. Certain gas rich meteorites seem to have been exposed to the solar wind before assembly, and there are nuclear track records of $\geq$ 1-MeV particles in some of these (*39*). The best case for cosmogenic nuclide production before compaction in a meteorite is provided by inclusions (xenoliths) in the chondrite St. Mesmin (*40*).

The number of known meteorites is rapidly multiplying, because of the large numbers of objects being found in "blue ice" regions of the Antarctic ice sheet. We are particularly interested in them because they are "old." From the evidence of cosmogenic nuclides, it appears that nearly all of them fell to earth more than 3×10^4 years ago (*41*) and generally between 1×10^5 and 7×10^5 years ago. Some iron meteorites have been on the earth longer; Tamarugal, for example, has a terrestrial age of $\sim 2 \times 10^6$ years (*37*) and is the oldest we know.

Cosmic spherules and cosmic dust. The cosmic spherules found in deep-sea sediments have long been known, from their composition, to be of extraterrestrial origin. They are comparatively abundant (1 part in 10^7) in deep-sea sediments because of the slow rate of sedimentation of terrestrial materials there. These spherules must include materials from the meteoroids that never reach the earth's land surface (*42, 43*). The main uncertainty about their makeup is whether they are mostly ablation droplets from large meteoroids or small meteoroids that have undergone partial or total fusion. Deep-sea sediment cores can provide a continuous record of the intensity and nature of incoming extraterrestrial material for hundreds of millions of years (*43, 44*).

Brownlee and his co-workers (*45*) have collected small (~ 10 micrometers), fluffy, unaltered particles in the stratosphere that seem to be of cometary origin. These particles, whose survival was predicted by Öpik (*46*), are often chondritic in composition, but much less dense and crystalline than the carbonaceous chondrites collected on the earth's surface. Solar wind noble gases have been detected in them (*47*), verifying their extraterrestrial origin, but the small amount of material collected so far precludes measuring any cosmic-ray effects.

History of the Cosmic Rays

Many targets bombarded by the cosmic rays have relatively simple exposure histories that can be used to study the irradiating particles. Tree rings, meteorites, lunar rocks, and parts of Surveyor III returned by the Apollo 12 astronauts are examples. Concentrations of radioactive and stable cosmogenic nuclides provide data for determining fluxes of SCR and GCR particles, and track densities provide information on the heavy nuclei.

Solar cosmic rays. Indirect measurements of SCR particle flux by ionization chambers or radio-wave absorption over the polar caps extend back to 1936, but direct measurement by particle detectors in satellites began only in 1960 (*1*). The SCR record in meteorites usually is removed by ablation during passage through the earth's atmosphere, but the record in the lunar samples is well preserved.

The depth-activity profiles of SCR-produced radionuclides are clearly evident in the surface layers of the returned lunar rocks. Generally the chemistries and cross sections used to derive mean fluxes and spectra of SCR particles, and the corrections for GCR production, are reasonably well known. The activities of short-lived radionuclides (for example, 78-day ^{56}Co and 35-day ^{37}Ar) produced in lunar rocks by solar protons were found to be in good agreement with those from satellite-measured proton fluxes for the solar flares (*8, 48*). The activities measured for ^{22}Na (2.6-years), ^{55}Fe (2.7-years), and ^{3}H (12.3-years) were made mainly by protons emitted before direct satellite measurements and, along with

Table 2. Average solar-proton fluxes over various time periods as determined from lunar radioactivity measurements. Abbreviation: SPME, solar proton monitor experiment (*78*).

Period	Data source	Reference	Fluxes (protons cm^{-2} sec^{-1})			
			$E >$ 10 MeV	$E >$ 30 MeV	$E >$ 60 MeV	$E >$ 100 MeV
1965 to 1976	SPME	(*8*)	90	30	8	
1954 to 1964	^{22}Na, ^{55}Fe	(*8*)	380	140	60	26
10^4 years	^{14}C	(*52*)		70	26	9
3×10^5 years	^{81}Kr	(*53, 54*)			18	9
10^6 years	^{26}Al	(*50*)	70	25	9	3
5×10^6 years	^{53}Mn	(*50*)	70	25	9	3

the relative intensities inferred from indirect measurements, were used to determine solar proton fluxes for the 1954 to 1964 solar cycle (*8*). The fluxes for the two most recent solar cycles were adopted from satellite measurements or determined from lunar radioactivities (*8*) (Table 2).

Several long-lived radionuclides are used to study past SCR fluxes: ^{14}C (5730 years), ^{59}Ni (8×10^4 years), ^{81}Kr (2.1×10^5 years), ^{26}Al (7.3×10^5 years) and ^{53}Mn (3.7×10^6 years). In lunar rocks with long exposure ages, the radionuclides can tell us about fluxes one to two half-lives before the present. The nuclides are produced mainly by solar protons, except ^{59}Ni, which is made mainly by solar alpha particles. On the basis of lunar ^{59}Ni activities and satellite measurements of solar alpha particles, Lanzerotti *et al.* (*49*) concluded that long-term and current solar alpha particle fluxes are comparable to within a factor of 4.

For the last 0.5×10^6 to 10×10^6 years, ^{26}Al and ^{53}Mn activities indicate relatively little change in the average fluxes of solar protons. The solar proton fluxes given in Table 2 are the values we prefer and are based on measurements from lunar rocks with a variety of exposure ages (*50*). Bhandari *et al.* (*51*) measured ^{26}Al activities in four rocks with exposure ages ranging from 0.5 to 3.7 million years and concluded that the average solar proton fluxes during the last 0.5 to 1.5 million years have varied less than ± 25 percent; their inferred fluxes are about three times those reported by Kohl *et al.* (*50*), however. The fluxes measured during the last few decades and the last few million years are similar, indicating that current solar activity is not atypical of what it has been in the past.

The activities of ^{14}C and ^{81}Kr indicate that average SCR fluxes for the last 10^4 and 10^5 years were considerably higher than they were during the last 10^6 years (Table 2). The ^{14}C measurements of Boeckl (*52*) for six depths in a lunar rock gave solar proton fluxes that are about three times those determined from ^{26}Al and ^{53}Mn data. Concentration-depth profiles of ^{81}Kr, measured by mass spectrometry in two lunar rocks, suggest that solar-proton fluxes above 60 MeV (the threshold energy for the main reactions producing ^{81}Kr) were considerably higher than those determined for the last 10^6 years (*53, 54*). There are, however, uncertainties in the ^{14}C- and ^{81}Kr-deduced fluxes (*54*).

Giant solar flares, much larger than any we have observed, might have occurred in the past. The tree ring record of ^{14}C seems to indicate that no flares more than ten times greater than those observed since 1956 have occurred since ~ 5000 B.C. The lunar data on ^{26}Al and ^{53}Mn set some limits on giant individual flares up to 10^7 years ago (*55*).

VH and VVH nuclei. The studies of tracks made by VVH and VH nuclei in meteorites and in lunar samples provide long-term average values of relative fluxes and energy spectra of nuclei for the Z interval 20 to 92 and in the energy region 0.5 to 2000 MeV per nucleon (*9, 56, 57*). The determination of absolute time-averaged fluxes of VH and VVH nuclei is not yet possible because of the lack of an independent measure of time; the inferences are somewhat model dependent. At low energies (< 10 MeV per nucleon), the duration of irradiation is controlled by erosion; in the high-energy region (> 100 MeV per nucleon), fragmentation, resulting in changes in the exposure geometry, becomes important. But it is possible to select rocks with a predominantly single-stage irradiation.

The flux and spectrum of iron group nuclei with energies of 100 to 200 MeV per nucleon are similar to these observed today. The tracks were formed during different intervals over the last 10^9 years. For nuclei of $Z \geq 30$, the available data primarily refer to the VVH/VH abundance ratios in the energy region 100 to 1000 MeV per nucleon. The ratio is found to be $1.5\ (\pm\ 0.2) \times 10^{-3}$, which is in good agreement with the abundance ratios in the sun or primitive chondrites (*57*). The relative abundances of heavier nuclei in the four charge groups, Z 52 to 62, 63 to 75, 76 to 83, and 90 to 96, have been found to match well with the solar and cosmic abundances.

Below 50 MeV per nucleon, the VVH/VH ratio increases as one goes to lower energies. For heavy nuclei, ~ 40 MeV per nucleon is the dividing line; above that the flux is due mainly to GCR and below to SCR particles (*57*). The ratio increases down to energies of ~ 1 MeV per nucleon, reaching about 2×10^{-2}, which is about ten times higher than the solar ratio. Preferential acceleration of heavier nuclei at lower energy also has been observed in recent SCR events (*58*).

High densities of tracks have been observed in grains inside the "gas rich" meteorites (*39*). The grains also have high concentrations of solar wind implanted noble gases (*59*). They appear to have been irradiated ~ 4×10^9 years ago while in a regolith similar to that found now on the moon's surface (*60*). Carbonaceous chondrites also have grains with tracks made during the early history of the solar system (*56*). The ratios of VVH/VH nuclei irradiating these meteoritic grains have varied but within factors of 2 or 3.

Analyses of SCR track densities and gradients in grains from lunar cores show no evidence for periods as long as ~ 10^3 years with high flux of heavy nuclei during the last billion years or so (*61*). The shape of the energy spectrum of VH nuclei has remained remarkably similar for the epochs for which data are available.

Galactic cosmic rays. Most studies of GCR flux variations compare activities of radionuclides with different half-lives in meteoritic or lunar samples. Ratios of measured activities to those predicted by various models or to the concentrations of stable cosmogenic nuclides are used to look for variations in average fluxes over the mean lives of various radionuclides. Activities of ^{14}C and ^{10}Be in terrestrial samples have been used to study flux variations over shorter time intervals.

The orbits of only three meteorites are accurately known. They had low orbital inclinations and therefore were exposed not far from the earth's orbital plane. The activities of long-lived radionuclides in these and other meteorites agree well, indicating that almost all meteorites have been exposed to similar fluxes of GCR particles. The Malakal chondrite has an unusually high activity of ^{26}Al, which might be the result of irradiation by a high flux of cosmic-ray particles before about 2×10^6 years ago (*62*); the ^{53}Mn content, however, is normal (*38*). High activity ratios of short-lived (^{22}Na and ^{54}Mn) to long-lived (^{26}Al and ^{53}Mn) radionuclides in the Dhajala chondrite have been interpreted as being due to higher GCR fluxes at heliographic latitudes between 15° and 40°S than within ±15° of the ecliptic plane during solar minimum (*63*).

The activities of ^{22}Na (2.6 years), ^{46}Sc (84 days), and ^{54}Mn (312 days) have been measured in 24 meteorites which fell between 1967 and 1978 (*64*). The activities varied by factors of 2 or more, and the variations correlated with the sunspot cycle, with maximum activities at solar minimum. These results indicate that production rates for cosmogenic nuclides in meteorites can vary by up to factors of 3 between solar minimum and solar maximum.

Production rates for radionuclides with half-lives from 16 days (^{48}V) to 3.7×10^6 years (^{53}Mn) were calculated for iron meteorites and compared with experimental activities in the Aroos iron meteorite (*65*). The ratios of observed to calculated activities varied but did not show any systematic trend with half-life. These and other results for radioactivities in meteorites and lunar samples indicate that the fluxes of energetic GCR particles have varied less than about 25 to 50 percent during the last few million years and are similar to present fluxes.

Most studies of long-term GCR flux variations use iron meteorites or metallic (FeNi) phases of meteorites because they are chemically simple targets. Most of the radionuclides produced from iron have reaction threshold energies above 100 MeV, so that secondary particles are relatively unimportant and results from bombardments with accelerated particles can be used to predict production-rate ratios. Forman *et al.* (*66*) examined activities of ^{37}Ar (35 days) and ^{39}Ar (269 years) in metal from about 12 meteorites. They found that the ^{39}Ar activities were 10 to 18 percent higher than expected from the ^{37}Ar activities, a result consistent with long periods of reduced solar modulation during the last 500 years. Measurements of ^{39}Ar activities in meteorites that fell several centuries ago would help confirm the presence of higher GCR fluxes during the Maunder minimum. Activity ratios of ^{39}Ar to ^{36}Cl (3×10^5 years) measured in iron meteorites are within 10 percent of the production ratios measured in iron targets bombarded by high-energy protons (*67*); thus the flux of GCR particles during the last ~ 500 years is similar to the average flux over the last $\sim 5 \times 10^5$ years.

Other long-lived radionuclides, such as ^{26}Al, ^{53}Mn, and ^{40}K, are produced by such different reactions that the calculated production ratios are somewhat model sensitive. As discussed above, a pair of radioactive and stable nuclides that are produced by similar reactions can be used to obtain exposure ages. For iron meteorites, the ages determined from $^{39}Ar/^{38}Ar$, $^{36}Cl/^{36}Ar$, and $^{26}Al/^{21}Ne$ ratios are usually similar, but those from $^{40}K/^{41}K$ ratios are usually about 50 percent higher (*68*). The differences cannot easily be explained by meteorite orbital changes $\sim 10^6$ to 10^7 years ago or space erosion (*68*). Thus, the flux of the cosmic rays to which iron meteorites were exposed during the past 10^6 years appears to have been roughly 50 percent more intense than the average for the last 10^9 years.

In stone meteorites, production rates of cosmogenic nuclides can vary considerably. Several investigators developed methods for determining exposure ages that include corrections for shielding effects due to different sizes and shapes of meteorites (*31, 69*). Studies (*33*) of radionuclides and cosmogenic neon in meteorites, including several with short exposure ages, indicate that the average GCR flux producing ^{26}Al in meteorites for the last 10^6 years could have been significantly greater (~ 40 percent) than that for ^{53}Mn over the last $\sim 5 \times 10^6$ years. The reactions that produce these two radionuclides have low threshold energies, so that this flux ratio involves lower energy particles than that for reactions in iron meteorites.

In addition to GCR flux changes, shielding changes due to multiple collisions or other causes could alter cosmogenic-nuclide production rates and apparent exposure ages, especially in meteorites with long exposure histories. Some of our data, such as half-lives, may be in error. These sources must be considered and eliminated before concluding that GCR flux variations caused production-rate changes in meteorites.

A GCR flux change could be either solar or nonsolar in origin. The movement of the solar system through the galaxy or in and out of the galactic plane could cause long-term flux changes (*70*). Rare external events (nearby supernovae) or solar variations (a Maunder minimum) can cause short-term flux changes. Such rapid fluctuations would be difficult to detect in extraterrestrial samples but are observable in terrestrial samples.

The most interesting cosmogenic radionuclides in terrestrial samples are those like ^{10}Be, ^{14}C, ^{32}Si, and ^{36}Cl, which are mainly made in the earth's atmosphere and which have half-lives that are long in comparison to the time scales for their removal from the atmosphere (*21*). These radionuclides produce "differential" records showing changes of production on a short time scale in organic matter, marine sediments, or glaciers that can be dated by independent techniques (for example, dendrochronology, geophysical events like magnetic reversals, or natural radioactivity). Most other radionuclides in the terrestrial environment yield results that are long-term averages only, like those in meteorites, because they mainly originate in interplanetary space (^{53}Mn) or reside in the atmosphere (^{39}Ar or ^{81}Kr).

The activities of ^{10}Be have been measured in deep-sea sediment cores, sections of which have been dated by paleomagnetic stratigraphy or by thorium isotope methods. Other chemical and physical properties of the cores were determined so that ^{10}Be concentrations could be converted to production rates (*71*). The ^{10}Be content varies, mainly because of changes in sedimentation rates but also possibly because of climatic changes or reversals or other variations in the earth's magnetic field. The inferred global ^{10}Be production rates for the last 2.5×10^6 years have varied by less than ±30 percent when averaged for periods of 10^5 years and less than ±10 percent for periods longer than 2×10^5 years. Studies of large diameter sediment cores from the equatorial Pacific Ocean indicate that, during the last 10^6 years, the global ^{10}Be production rate could have changed once by as much as 30 ± 7 percent, averaged over $\sim 10^5$ years, and had perhaps three or four smaller excursions with amplitudes of < 20 percent (*72*).

As discussed above and shown in Fig. 4, the measured ^{14}C activities in dated tree rings can be resolved into two components: one slowly varying because of geomagnetic field changes and one rapidly oscillating. The rapid variations (called Suess wiggles) have amplitudes of 1 to 2 percent and a prominent 200-year periodicity (*18*). These amplitudes agree with those predicted for changes in GCR fluxes due to extremes in solar modulation (*7*). The terrestrial ^{14}C data provide the sharpest limit available on short-term spikes, or sudden shifts, in the particle flux in the inner solar system. Because atmospheric $^{14}CO_2$ is a small part of the total ^{14}C reservoir, and because the transfer of CO_2 to other, larger parts of the reservoir is slow (*73*), a sharp spike or shift in production is well displayed in the record. Thus the production of ^{14}C by nuclear weapons testing in the early 1960's produced a quick doubling of atmospheric ^{14}C which has now decayed to a much lower level. The Suess wiggles are believed to provide evidence for long periods of unusual solar activity (*5, 18, 74*), and the magnitudes are consistent with the expected variations in production rates for a periodicity in solar activity of ~ 200 years (*7*). A larger change in the low-energy (< 1 GeV) proton flux is not ruled out, because such protons only reach the earth's atmosphere in the polar regions.

Conclusions

The most definite evidence for time variations of the cosmic rays near the earth is provided by studies of SCR products in lunar samples. The ^{14}C data seem to require a rather high proton flux on a scale of 10^4 years; limited ^{81}Kr data suggest something similar for as long as a few hundred thousand years. Over the longer periods, represented by ^{26}Al and ^{53}Mn, the flux seems to have been lower, on the average more like the present, if we knew how to define a present-day average.

We have several lines of evidence for the GCR intensity in space 1 to 3 AU from the sun. The best is ^{14}C variations in wood, which indicate a strong solar modulation effect leading to a large change in the global production of ^{14}C with an average period of about 200 years. These variations exceed in magnitude, but are similar to, solar modulation effects observed during the last few decades. The last such period of unusual solar activity, the Maunder minimum, apparently also caused enhanced production of ^{39}Ar in meteorites.

On a longer time scale the classical result is that there has been no change in the time-averaged GCR flux near the earth within some error on the order of 30 to 40 percent. Variations might well be expected either from changes in solar modulation on longer time scales, or in the sun's location in the galaxy (in or out of spiral arms). On a time scale of 10^5 to 10^7 years, we see effects that may be due to such changes, but other possibilities have not been eliminated.

On a 10^9-year scale, data on cosmogenic ^{40}K in iron meteorites require an increase in cosmic-ray flux toward the present; over ~ 10^9 years, the average is about one-third lower than that of the last 10^6 years. We cannot yet be sure whether this is a chapter in the history of meteorites or that of the cosmic rays.

Track and noble gas studies indicate that cosmic rays were present in the solar system near its beginning, with energy and charge spectra much like they are today. We may learn more from comparisons of the relative intensities of the solar wind, SCR, and GCR.

Studies of SCR products in lunar samples allow us to measure rates of meteorite impact, gardening, and rock fragmentation on the moon's surface. Gardening due to impact occurs to depths on the order of 10 cm in a few million years. Surfaces of lunar rocks are eroded at rates of ~ 1 mm per 10^6 years.

Meteorites are broken out of larger bodies, again by impact processes, on time scales of ~ 10^5 to 10^9 years. Meteorites that have been in unusual orbits may show some differences in the GCR fluxes.

With the development of more sensitive techniques to measure cosmogenic radionuclides, we can expect to increase greatly the range and precision of the data available to us. The study of ^{10}Be in terrestrial ice cores may provide a detailed look at time variations in a range of time scales. The use of two or more isotopes (for example, ^{10}Be and ^{26}Al) can remove uncertainties in interpretation. Deep-sea sediments and the cosmic spherules they contain, and also Antarctic meteorites, will provide other important windows on the past.

References and Notes

1. M. A. Pomerantz and S. P. Duggal, *Rev. Geophys. Space Phys.* **12**, 343 (1974).
2. J. A. Simpson, *Astronaut. Aeronaut.* **16**, (No. 7/8), 96 (1978).
3. R. E. Lingenfelter, *Int. Cosmic Ray Conf.* **14**, 135 (1979).
4. H. Moraal, *Space Sci. Rev.* **19**, 845 (1976).
5. J. A. Eddy, *Science* **192**, 1189 (1976).
6. M. Garcia-Munoz and J. A. Simpson, personal communication.
7. G. Castagnoli and D. Lal, *Radiocarbon* **22**, 133 (1980).
8. R. C. Reedy, *Proc. Lunar Sci. Conf.* **8**, 825 (1977).
9. D. Lal, *Space Sci. Rev.* **14**, 3 (1972).
10. M. A. I. Van Hollebeke, L. S. Ma Sung, F. B. McDonald, *Sol. Phys.* **41**, 189 (1975).
11. R. C. Reedy and J. R. Arnold, *J. Geophys. Res.* **77**, 537 (1972).
12. R. L. Fleischer, P. B. Price, R. M. Walker, *Nuclear Tracks in Solids* (Univ. of California Press, Berkeley, 1975).
13. T. W. Armstrong and R. G. Alsmiller, Jr., *Proc. Lunar Sci. Conf.* **2**, 1729 (1971).
14. R. E. Lingenfelter, E. H. Canfield, V. E. Hampel, *Earth Planet. Sci. Lett.* **16**, 355 (1972).
15. T. P. Kohman and M. L. Bender, in *High-Energy Nuclear Reactions in Astrophysics*, B. S. P. Shen, Ed. (Benjamin, New York, 1967), p. 169; B. M. P. Trivedi and P. S. Goel, *J. Geophys. Res.* **78**, 4885 (1973); M. Honda, *ibid.* **67**, 4847 (1962).
16. D. Lal, *Philos. Trans. R. Soc. London Ser. A* **285**, 69 (1977).
17. W. F. Libby, *Radiocarbon Dating* (Univ. of Chicago Press, Chicago, ed. 2, 1955).
18. H. E. Suess, *Radiocarbon* **22**, 200 (1980).
19. ———, *Endeavour* **4**, 113 (1980).
20. J. A. Eddy, *Clim. Change* **1**, 173 (1977).
21. D. Lal and B. Peters, *Handb. Phys.* **46** (part 2), 551 (1967).
22. S. Tanaka, K. Sakamoto, J. Takagi, M. Tsuchimoto, *Science* **160**, 1348 (1968).
23. H. T. Millard, Jr., *ibid.* **147**, 503 (1965); K. Nishiizumi *et al.*, *Earth Planet. Sci. Lett.* **52**, 31 (1981).
24. R. A. Muller, *Science* **196**, 489 (1977); C. L. Bennett *et al.*, *ibid.* **198**, 508 (1977); G. M. Raisbeck, F. Yiou, M. Fruneau, J. M. Loiseaux, *ibid.* **202**, 215 (1978); A. E. Litherland, *Annu. Rev. Nucl. Part. Sci.* **30**, 437 (1980).
25. G. M. Raisbeck, F. Yiou, M. Fruneau, M. Lieuvin, J. M. Loiseaux, *Nature (London)* **275**, 731 (1978); G. M. Raisbeck *et al.*, *Geophys. Res. Lett.* **6**, 717 (1979); G. M. Raisbeck *et al.*, *Earth Planet. Sci. Lett.* **51**, 275 (1980); G. M. Raisbeck, F. Yiou, M. Fruneau, J. M. Loiseaux, M. Lieuvin, *ibid.* **43**, 237 (1979).
26. F. Hörz, R. V. Gibbons, D. E. Gault, J. B. Hartung, D. E. Brownlee, *Proc. Lunar Sci. Conf.* **6**, 3495 (1975); M. Wahlen *et al.*, *ibid.* **3**, 1719 (1972).
27. C. Behrmann *et al.*, *ibid.* **4**, 1957 (1973).
28. J. N. Goswami and D. Lal, *ibid.* **10**, 1253 (1979).
29. Y. Langevin and J. R. Arnold, *Annu. Rev. Earth Planet. Sci.* **5**, 449 (1977); ———, K. Nishiizumi, *J. Geophys. Res.* **87**, 6681 (1982).
30. H. Voshage and H. Feldmann, *Earth Planet. Sci. Lett.* **45**, 293 (1979).
31. G. F. Herzog and P. J. Cressy, Jr., *Geochim. Cosmochim. Acta* **38**, 1827 (1947); P. J. Cressy, Jr., and D. D. Bogard, *ibid.* **40**, 749 (1976).
32. R. C. Finkel, C. P. Kohl, K. Marti, B. Martinek, L. Rancitelli, *ibid.* **42**, 241 (1978).
33. K. Nishiizumi, S. Regnier, K. Marti, *Earth Planet. Sci. Lett.* **50**, 156 (1980); O. Müller, W. Hampel, T. Kirsten, G. F. Herzog, *Geochim. Cosmochim. Acta* **45**, 447 (1981).
34. J. Crabb and L. Schultz, *Geochim. Cosmochim. Acta* **45**, 2151 (1981).
35. E. Öpik, *Interplanetary Encounters* (Elsevier, Amsterdam, 1976); J. R. Arnold, *Astrophys. J.* **141**, 1536 (1965).
36. T. Kirsten, D. Krankowsky, J. Zähringer, *Geochim. Cosmochim. Acta* **27**, 13 (1963); E. Anders, *Science* **138**, 431 (1962).
37. C. Chang and H. Wänke, in *Meteorite Research*, P. M. Millman, Ed. (Reidel, Dordrecht, 1969), p. 397.
38. K. Nishiizumi, *Earth Planet. Sci. Lett.* **41**, 91 (1978).
39. D. Lal and R. S. Rajan, *Nature (London)* **223**, 269 (1969); P. Pellas, G. Poupeau, J. C. Lorin, H. Reeves, J. Audouze, *ibid.*, p. 272.
40. L. Schultz and P. Signer, *Earth Planet. Sci. Lett.* **36**, 363 (1977).
41. E. L. Fireman, *Proc. Lunar Planet. Sci. Conf.* **11**, 1215 (1980).
42. D. E. Brownlee, in *Cosmic Dust*, J. A. M. McDonnell, Ed. (Wiley, Chichester, 1978), p. 295.
43. M. T. Murrell, P. A. Davis, Jr., K. Nishiizumi, H. T. Millard, Jr., *Geochim. Cosmochim. Acta* **44**, 2067 (1980).
44. D. W. Parkin, R. A. L. Sullivan, J. N. Andrews, *Philos. Trans. R. Soc. London Ser. A* **297**, 495 (1980).
45. D. E. Brownlee, in *Protostars and Planets*, T. Gehrels, Ed. (Univ. of Arizona Press, Tucson, 1978), p. 134; ———, D. A. Tomandl, E. Olszewski, *Proc. Lunar Sci. Conf.* **8**, 149 (1977).
46. E. Öpik, *Publ. Tartu Astrofiz. Obs.* **29**, 51 (1937).
47. R. S. Rajan, D. E. Brownlee, D. Tomandl, P. W. Hodge, H. Farrar IV, R. A. Britten, *Nature (London)* **267**, 133 (1977); B. Hudson, G. J. Flynn, P. Fraundorf, C. M. Hohenberg, J. Shirck, *Science* **211**, 383 (1981).
48. R. C. Finkel *et al.*, *Proc. Lunar Sci. Conf.* **2**, 1773 (1971).
49. L. J. Lanzerotti, R. C. Reedy, J. R. Arnold, *Science* **179**, 1232 (1973).
50. C. P. Kohl, M. T. Murrell, G. P. Russ III, J. R. Arnold, *Proc. Lunar Planet. Sci. Conf.* **9**, 2299 (1978).
51. N. Bhandari, S. K. Bhattacharya, J. T. Padia, *Proc. Lunar Sci. Conf.* **7**, 513 (1976).
52. R. S. Boeckl, *Earth Planet. Sci. Lett.* **16**, 269 (1972).
53. A. Yaniv, K. Marti, R. C. Reedy, in *Lunar and Planetary Science XI* (Lunar and Planetary Institute, Houston, 1980), p. 1291.
54. R. C. Reedy, *Proc. Conf. Ancient Sun* (1980), p. 365.
55. R. E. Lingenfelter and H. S. Hudson, *ibid.*, p. 69.
56. J. N. Goswami, D. Lal, J. D. Macdougall, *ibid.*, p. 347.
57. D. Lal, *Philos. Trans. R. Soc. London Ser. A* **277**, 395 (1974); N. Bhandari, J. N. Goswami, D. Lal, A. S. Tamhane, *Astrophys. J.* **185**, 975 (1973); N. Bhandari and J. T. Padia, *Science* **185**, 1043 (1974).
58. E. K. Shirk, *Astrophys. J.* **190**, 695 (1974).
59. P. Eberhardt, J. Geiss, N. Grögler, *J. Geophys. Res.* **70**, 4375 (1965); H. Wänke, *Z. Naturforsch. Teil A* **20**, 946 (1965).
60. K. R. Housen, L. L. Wilkening, C. R. Chapman, R. Greenberg, *Icarus* **39**, 317 (1979).
61. G. Crozaz, *Proc. Conf. Ancient Sun* (1980), p. 331.
62. P. J. Cressy, Jr., and L. A. Rancitelli, *Earth Planet. Sci. Lett.* **22**, 275 (1974).
63. N. Bhandari, S. K. Bhattacharya, B. L. K. Somayajulu, *Earth Planet. Sci. Lett.* **40**, 194 (1978).
64. J. C. Evans, J. H. Reeves, L. A. Rancitelli, D. D. Bogard, *J. Geophys. Res.* **87**, 5577 (1982).

65. J. R. Arnold, M. Honda, D. Lal, *J. Geophys. Res.* **66**, 3519 (1961).
66. M. A. Forman, O. A. Schaeffer, G. A. Schaeffer, *Geophys. Res. Lett.* **5**, 219 (1978).
67. O. A. Schaeffer and D. Heymann, *J. Geophys. Res.* **70**, 215 (1965).
68. W. Hampel and O. A. Schaeffer, *Earth Planet. Sci. Lett.* **42**, 348 (1979).
69. G. F. Herzog and P. J. Cressy, Jr., *Geochim. Cosmochim. Acta* **41**, 127 (1977).
70. M. A. Forman and O. A. Schaeffer, *Rev. Geophys. Space Phys.* **17**, 552 (1979).
71. B. L. K. Somayajulu, *Geochim. Cosmochim. Acta* **41**, 909 (1977); S. Tanaka and T. Inoue, *Earth Planet. Sci. Lett.* **45**, 181 (1979).
72. P. Sharma and B. L. K. Somayajulu, *Earth Planet Sci. Lett.* **59**, 235 (1982).
73. J. R. Arnold and E. C. Anderson, *Tellus* **9**, 28 (1957).
74. M. Stuiver, *J. Geophys. Res.* **66**, 273 (1961).
75. M. Garcia-Munoz, G. M. Mason, J. A. Simpson, *Astrophys. J.* **202**, 265 (1975).
76. C. O. Bostrom *et al.*, *Solar Geophysical Data* (1967–1973), monthly reports.
77. M. Wahlen, R. C. Finkel, M. Imamura, C. P. Kohl, J. R. Arnold, *Earth Planet. Sci. Lett.* **19**, 315 (1973).
78. K. Nishiizumi, M. Imamura, C. P. Kohl, M. T. Murrell, J. R. Arnold, G. P. Russ III, *Earth Planet. Sci. Lett.* **44**, 409 (1975); K. Nishiizumi, personal communication.
79. We thank M. Honda, K. Marti, K. Nishiizumi, H. E. Suess, M. Garcia-Munoz, and J. A. Simpson for valuable discussions and for unpublished results and figures. Supported in part by NASA grant NSG-7027 and NASA work order 14,084.

Impact of Genetic Manipulation on Society and Medicine

Arno G. Motulsky

Summary. Human beings have been manipulating the genetic characteristics of plants and animals since the introduction of agriculture. Indirect manipulation of human genes occurred with widespread use of public health and medical measures that preserve genes causing disease. The production of biologicals by DNA technology raises few ethical problems. Predictive medicine in which genetic markers (including DNA variants) are used for antenatal and preclinical diagnosis of genetic diseases and susceptibilities poses new questions of confidentiality, private versus societal goals, and self-determination. When normal DNA is used to treat the somatic cells of patients with hemoglobinopathies and other genetic diseases, no new ethical problems arise beyond those presented by any novel theory. In contrast, manipulation of DNA in human fertilized eggs would constitute a qualitative departure from previous therapies since this would affect future generations. In order to be able to make wise decisions on these matters the public must be well informed. Thus, formal and informal education in human biology and genetics must be improved at all levels.

The rapid development of molecular genetics and particularly the introduction of recombinant DNA technology have elicited much interest among scientists, physicians, and the public in general. The realization that scientists might be able to manipulate the heredity not only of lower organisms but also of our own species has led to much soul searching. Some observers maintain that mankind is at the threshold of new powers that are unlike any innovations ever faced before.

Where do we stand? Scientists and physicians need to be well informed about the current status of genetic manipulation so as to be able to inform the public regarding the scientific facts. Sometimes incomplete knowledge and lack of understanding of various issues in this rapidly evolving subject have led to unwarranted emotional reactions and ill-advised resolutions designed to block the progress of investigative activity.

Genetic Manipulation in the Past

Genetic manipulation is not a new development. For several thousand years, human beings have attempted to control their environment by influencing the genetic characteristics of other species. The domestication of wild plants and animals is an example of genetic manipulation with the aim of producing better and more food. Other examples include the improvement of egg and milk yields from domestic animals. The domestication of dogs shows that even behavior has been manipulated genetically. Hunting dogs, herding dogs, and watch dogs are only a few of the many kinds that were produced purposefully by breeding for specific behavioral characteristics—a form of genetic manipulation.

Genetic manipulation by design has rarely been practiced in our own species. However, unplanned genetic selection for intelligence probably occurs frequently. Marital partners resemble each other in intelligence (at least as measured by IQ tests) because of assortative mating for this trait (*1*). While the exact contribution of heredity to IQ remains unknown, most informed observers accept that genes contribute to the variability of IQ. Therefore, the elevated IQ levels observed on the average among offspring of intelligent parents are an example of genetic selection based on social customs. Such an assertion does not deny that there is a significant environmental component under these circumstances. However, even if the genetic contribution to intelligence is relatively small, assortative mating for IQ would be expected to concentrate high IQ genes among the offspring of gifted couples.

Human breeding by design for high intelligence was recently suggested by a California millionaire who arranged to use sperm from Nobel Prize winners in the sciences for artificial insemination of self-selected volunteer women. One would expect statistically that the offspring of such a procedure would be more intelligent than the average. No other predictions regarding future achievements could be made. Presumably, such voluntary private undertakings on a small scale would cause few social problems and would have no significant effects on the human gene pool. However, attempts by governments to control human breeding must be viewed with alarm—particularly since such efforts would interfere with civil liberties

The author is professor of medicine and genetics and director of the Center for Inherited Diseases at the University of Washington, Seattle 98195. This article is based on a paper published in German in *Medizin und Gesellschaft—Ethische Verantwortung und Arztliches Handeln*, G. A. Martini, Ed. (Umwelt und Medizin, Frankfurt, 1982, ISBN 3-92-1324-01-5).